JET-R(96)07

Validation of a New Mixed Bohm/gyro-Bohm Transport Model on Discharges of the ITER Data-Base

M Erba, A Cherubini, V V Parail,
E Springmann, A Taroni.

JET Joint Undertaking, Abingdon, Oxfordshire, OX14 3EA, UK.

July 1996

ABSTRACT

A new model is proposed for heat transport in the L-mode regime, which is the commonest regime of operation of Tokamaks. This model is directly derived from a previous Bohm-like model tested on JET discharges by adding a gyro-Bohm-like part that is peaked in the plasma centre and dominates the heat flux in small machines. This model has been successfully tested on data from different experiments from the newly established ITER profile data-base

1. INTRODUCTION

The recent set-up of the ITER profile database [1] has greatly increased the possibility of testing transport models on a wide range of plasma parameters simulating discharges from different machines.

In this work we present results of the simulation of L-mode discharges contained in the ITER profile database from JET, DIIID, TFTR and JT-60U and also of discharges from the ASDEX [2,3] and START [4] that we obtained directly from the local databanks.

In order to devise a suitable model for such a wide database we will follow the usual approach based on dimensional analysis [5]. It is well known that the coefficient of thermal and particle diffusion in plasmas can be written in the form :

$$\chi = \chi_0 \cdot F(x_1, x_2, \ldots) \qquad 1)$$

where χ_0 posesses the correct physical dimensions $\left[l^2 t^{-1}\right]$ while F is a function of properly chosen dimensionless plasma parameters. For χ_0 the usual Bohm expression cT_e / eB is used and the dimensionless parameters entering the function F are the plasma normalized gyroradius $\rho^* = m_i^{1/2} T_e^{1/2} / (eaB)$, the effective collisionality parameter $\nu^* = (R/r)^{3/2} qR\nu_e (m_e / 2T_e)^{1/2}$ (ν_e being the electron-ion collision frequency), the plasma beta $\beta = 8\pi p / B_0^2$, the safety factor q, etc.. The scaling of the function F with the normalized gyro-radius is directly related to the scale length of the turbulence underlying anomalous transport.

When F is linearly dependent on ρ^* the scale-length of plasma turbulence is a microscopic quantity of the order of the plasma gyro-radius. In this case the diffusivity depends only on local plasma parameters and transport properties are said to be gyro-Bohm-like. This is the case of drift-wave instabilities driven by finite temperature and density gradients in the plasma [6]. More recently drift-wave instabilities have been studied in the toroidal geometry typical of Tokamak configurations, showing that turbulence might be characterised by a large correlation length in the radial direction that scales with the plasma minor radius due to toroidal coupling [7]. Transport models related to this kind of modes are said to be Bohm-like and correspond to the case when F is independent of ρ^* .

It is also worth mentioning that when F has an inversely proportional dependence on ρ^* the correlation length is much larger than the plasma minor radius and could be related to the presence of stochastic magnetic field lines in the plasma [8].

Until now we have studied models with either a pure Bohm-like [9] or a pure gyro-Bohm-like [2] nature, finding that a simple Bohm-like model [9] is very successful in simulating L-mode JET discharges. This appeared to be in good agreement with experiments carried out in JET [10] and TFTR [11] showing effective transport properties (electrons plus ions) to be Bohm-like in these machines.

More recently the results of several ρ^* -scaling experiments carried out in DIIID where it has been possible to study separately the electron and ion transport due to low density have been published [8]. In discharges with predominant electron heating (ECH) and in discharges with predominant ion heating (NBI) transport properties have turned out to be gyro-Bohm-like for the electrons, while for the ions an intermediate scaling between stochastic and Bohm-like was found. Previous results from JET and TFTR have been explained by the fact that NBI heating had been used and ions had been predominantly heated. In this situation the ion component was more important in the total power balance and the Bohm-like character was more pronounced in effective transport properties.

The DIIID results suggest that the nature of transport cannot be described using a single scaling with the normalized gyro-radius, so that a model with combined Bohm/gyro-Bohm character might be required to explain the results from machines with different parameters.

As we will show in section 4) a clear result of our simulations is that using pure Bohm-like or pure gyro-Bohm-like models it is not possible to reproduce all the discharges of the selected database; in particular the Bohm-like model fails in small experiments with low toroidal field (ASDEX,START), while the gyro-Bohm like model fails in large experiments with high toroidal field (TFTR). The different behaviour of the models in different experiments can be related to the variation of the ρ^* parameter.

A simple solution to this problem is the development of a mixed model containing a Bohm-like and a gyro-Bohm-like term, which is equivalent to expanding in a Taylor series the function F in equation 1) in terms of the small parameter ρ^*:

$$F \propto 1 + \varepsilon \cdot \rho^* \qquad 2)$$

where ε is a function of dimensionless parameters (except ρ^*) to be determined empirically.

At this point two important general considerations are necessary.

First of all we observe that since the ρ^* parameter increases from large to small machines, transport properties undergo a transition from a Bohm-like regime to a gyro-Bohm-like regime if ρ^* becomes larger than $(1/\varepsilon)$.

Secondly, since the normalized gyro-radius depends on the square root of the local temperature $\rho^* \propto T_e^{1/2}$, there is a natural tendency for the gyro-Bohm term to be more important in the plasma centre with respect to the Bohm-like term when other functional dependencies are similar.

Starting from expansion 2) we will develop an expression of the diffusion coefficient with the following form:

$$\chi_{e,i} = \chi_{Be,i} + \chi_{gBe,i} \qquad 3)$$

where $\chi_{Be,i}$ is the diffusivity of the Bohm-like model [9] and for the gyro-Bohm-like term we use the following expression for both ions and electrons:

$$\chi_{gB} = \alpha_{gB} \cdot \frac{cT_e}{eB_t} \cdot L_{Te}^{*-1} \cdot \rho^* \qquad 4)$$

$$\rho^* = \frac{2^{1/2} \cdot M^{1/2} \cdot c \cdot T_e^{1/2}}{e \cdot B_t} \qquad 5)$$

where α_{gB} is an empirical constant common to electrons and ions. The additional gyro-Bohm-like term helps to improve the performance of the model in small machines where it is dominant; results of the simulations remain very good in large machines where the Bohm-like term is dominant, and in the DIIID experiment where the two terms are comparable.

2. BOHM, GYRO-BOHM AND MIXED MODELS.

In the past a simple empirical local transport model of the Bohm type has made it possible to simulate successfully the ion and electron temperature profiles of a number of relevant JET discharges [9,12]. The expression of the model in dimensionless form is:

$$\chi_e = \alpha_B \cdot \frac{cT_e}{eB_t} \cdot L_{pe}^{*-1} \cdot q^2 \cdot a \qquad 6)$$

$$L_{pe}^* = \frac{p_e}{a|\nabla p_e|} \qquad 7)$$

In machines different from JET transport properties were found to have a different character: recent analysis has shown the pure Bohm-like model to fail in the simulation of discharges from the START experiment [4], while other gyro-Bohm-like models were more successful.

Previous simulations of ASDEX discharges [3] had shown that a pure gyro-Bohm-like model was working better than the Bohm-like one:

$$\chi_e = \alpha_{gB} \cdot \frac{cT_e}{eB_t} \cdot L_{pe}^{*-1} \cdot q^2 \cdot \rho^* \qquad 8)$$

In order to account for different experiments using a single transport model we modify the pure Bohm model for L-mode by adding a simple gyro-Bohm term to both the electron and the ion conductivity; for the gyro-Bohm term we use the same expression for ions and electrons so that the complete expression of the model is:

$$\chi_e = \chi_{e,B} + \chi_{gB} \qquad 9)$$

$$\chi_i = 2 \cdot \chi_{e,B} + \chi_{gB} \qquad 10)$$

where for $\chi_{e,B}$ we use the same expression of the pure Bohm-like model eq. 6) with the numerical coefficient $\alpha_B = 2.5 \cdot 10^{-4}$ and for χ_{gB} we use eq. 4) with $\alpha_{gB} = 3.5 \cdot 10^{-2}$ (this choice will be justified in the next section by comparison with experimental data).

The mixed model can also be written as:

$$\chi_e = c_{gB} \cdot \frac{\sqrt{T_e}|\nabla T_e|}{B_t^2} + c_B \cdot a \cdot \frac{|\nabla p_e|}{n_e B_t} \cdot q^2 \qquad 11)$$

$$\chi_i = c_{gB} \cdot \frac{\sqrt{T_e}|\nabla T_e|}{B_t^2} + 2 \cdot c_B \cdot a \cdot \frac{|\nabla p_e|}{n_e B_t} q^2 \qquad 12)$$

where for the numerical constants of the Bohm-like and gyro-Bohm-like term we use $c_B = 2.5 \cdot 10^4$, $c_{gB} = 5.0 \cdot 10^8$.

As it can be seen in eqs. 9),10) the mixed model is made up of a term independent of ρ^* plus a term linearly dependent on ρ^*; by properly choosing the numerical coefficients it is possible to have a model that is predominantly Bohm-like as the dimensions of the machine and the toroidal field increase and ρ^* decreases, and predominantly gyro-Bohm-like in small machines with low toroidal field (ASDEX, START) where ρ^* is large. Furthemore, since in our model the gyro-Bohm-like term does not contain the q^2 dependence on the safety factor it is

not strongly increasing towards the plasma edge where the Bohm-like term dominates; the gyro-Bohm-like term in this way is naturally more important in the plasma centre, which has interesting consequences for the extension of the model to other regimes (see section 5). Finally, since the Bohm-like term is multiplied by 2 for the ions (see eqs. 9),10)), they will tend to have a more pronounced Bohm-like character and regimes will exist where electrons are predominantly gyro-Bohm-like and ions are predominantly Bohm-like.

3. SIMULATED DISCHARGES

In Table I we report the parameters of the discharges whose simulations we will present in this work.

Selected shots have been chosen out of a larger database of simulated discharges because they are representative of typical L-mode shots in different machines: only the START shot is in the ohmic saturated regime which we have shown to possess very similar characteristics to the L-mode regime [12]. The ASDEX discharges [3], the START discharges [5] and the two DIIID discharges 78283 and 78109 [8] are not available in the ITER database and have been taken from the local databanks.

The JET shots are two standard L-mode NBI heated discharges where the input power has been varied by a factor 2; these discharges are particularly well diagnosed and have been analysed with TRANSP [14] and successfully simulated with the Bohm-like model [12].

The DIIID shots 71384 and 71378 belong to an old ρ^* - scaling experiment performed in DIIID [15]; in this experiment electron and ion transport cannot be separated and electron temperature profiles only are available for this discharge. The results of the previous analysis of these experiments were shown to be not conclusive about the Bohm-like or gyro-Bohm-like nature of heat transport: this is in agreement with the idea presented in this paper that these discharges are in an intermediate regime between Bohm and gyro-Bohm scaling.

The DIIID shots 78283 and 78109 are L-mode NBI-heated discharges belonging to the most recent series of ρ^* - scaling experiments [8]. The analysis of these shots showed a gyro-Bohm-like scaling for electrons, a scaling of the ion transport intermediate between Bohm-like and stochastic and a Bohm-like scaling for effective transport.

The TFTR shot of Table I is a standard L-mode, NBI-heated discharge included in the ITER database. The JT-60U shots belong to a ρ^* - scaling experiment while the ASDEX shot does not belong to the ITER database and does not posess data for ion temperatures.

The START discharge is an ohmic shot that has not been included in the ITER data-base yet [5]. The main interest of this shot is that its parameters are very much separated from those of the other machines and the normalized gyro-radius ρ^* is much larger in this case. Unfortunately available data are poor: ion temperatures and Z_{eff} are not known (in our

simulations we will adopt the sensible guess Z_{eff}=2), and the electron density and temperature profiles have been measured only at few radial points. For these reasons the results of this simulation must be taken very carefully and can only be used as an indication of the general trend in transport properties when one goes from large to small machines.

4. SIMULATIONS RESULTS

Simulations using the transport models for the electron and ion heat diffusivity presented in section 2) have been carried out in a semi-predictive way using the 1 1/2 D transport code JETTO [16]: the density profiles, the Z_{eff} profiles, the power deposition profiles and the edge temperature have been prescribed using the values contained in the databases.

In the following we will show the simulations results in terms of the profiles of the electron and ion temperature that will be compared to the experimental profiles when these are available.

With the above choice of the numerical constants all the models provide a good fit of the JET data: this shows how difficult it is to distinguish between Bohm-like and gyro-Bohm-like models simulating discharges from a single experiment [9]. The results of the JET simulations are shown in Figs 1a,1b for electron and ion temperatures in the reference shot 19649, and in Figs. 2a,2b for electron and ion temperatures in shot 19691. As it can be seen the mixed model in these simulations behaves in a similar way to the pure Bohm-like model. This can be understood from Fig. 3 where the profiles of the Bohm-like and gyro-Bohm-like terms which make up this model are compared for the reference JET discharge: it is easily seen that the gyro-Bohm term is negligible all over the plasma column.

The predominancy of the Bohm-like term is even more pronounced in TFTR due to the large value of the toroidal field: in Figs. 4a-b we show the results of the simulation of an L-mode TFTR discharge from the ITER database. As we can see the pure Bohm-like and mixed models behave in a similar way, due to the small value of the gyro-Bohm-like term in the mixed model; the pure gyro-Bohm-like model badly overestimates both the electron and ion temperature profiles: this is a clear sign that the variation of transport properties from JET to TFTR is not adequately described by the gyro-Bohm scaling.

The results of the simulation of JT60-U discharges (see figs. 5a-b,6a-b) are not very different for the different models: however it can be seen that the mixed model is the most successful in all cases.

The results of the simulations of the DIIID discharges of the ITER database are shown in Figs. 7a-b, 8a-b. We observe that the pure Bohm-like model is overoptimistic, the pure gyro-Bohm-like model is overpessimistic while the mixed model is in agreement with experimental

profiles. The success of the mixed model in the DIIID discharges is due to the effect of the gyro-Bohm-like term, which is not negligible in the plasma centre in DIIID (see Fig. 9).

All the results of the simulation of discharges belonging to the ITER database can be understood in terms of the variation of the normalized gyro-radius: in Table II we show the central value of the ρ^* parameter defined in eq. 5) for reference discharges of the JET, TFTR, JT60-U, DIIID, Asdex and START experiments. It easy to see that this parameter is much larger in DIIID than in TFTR, explaining why the pure Bohm-like model is overoptimistic in START and the gyro-Bohm-like model is overoptimistic in TFTR. The mixed model on the other hand seems to contain Bohm-like and gyro-Bohm-like terms in the right balance and is successful in all simulated discharges of the ITER database.

The results from the DIIID shots belonging to the latest ρ^*-scaling experiments are shown in Figs. 10a-b and 11a-b.

Also in the case of ASDEX no data are available for the ion temperature profiles; in Figs. 12 we compare the profiles obtained with the three models with the experimental electron temperature profiles. As we can see the pure gyro-Bohm-like model gives the best results, the pure Bohm-like model fails while the mixed model is marginally compatible with the data.

Finally we have also carried out simulations of dicharges from the START experiment: in this case the experimental data available are far from complete, and we had to use sensible guesses for the value of Z_{eff} and for the radiated power in order to carry out the simulations. Furthemore the ion temperature is not measured while for the electron temperature only few radial data points are available.

From the simulation results, shown in Fig. 13, we deduce that the pure-Bohm-like model is definitely unsuccessful, that the mixed model overestimates the temperature while the pure gyro-Bohm-like model is in good agreement with data. Keeping into account the uncertainties related to this simulation, we consider these results as an indication that gyro-Bohm-like terms in the diffusion coefficient become dominant in small machines, in agreement with the variation of the ρ^* parameter (see Table II).

5. DISCUSSION

The results presented in the previous sections show that a mixed Bohm/gyro-Bohm model can be successful in simulating a large database of discharges from machines with very different plasma parameters. This is possible because the Bohm-like and gyro-Bohm-like terms become dominant in different machines according to the variation of the ρ^* parameter.

In fig. 14) we summarize the simulations of the ITER database discharges by plotting the relative deviation of the thermal energy :

$$\Delta = \frac{W_{th,sim} - W_{th,\exp}}{W_{th,\exp}} \qquad 13)$$

The results of heat transport modelling with the mixed model presented in this paper concern only L-mode discharges; however there are several indications that the same model with some modifications might be working in H-mode discharges too.

Since the Bohm-like term has a global dependence on plasma parameters and since at the L-H transition a global modification of the diffusion coefficient has been observed [17], it is natural to explain the improved confinement properties in H-mode by a reduction in the Bohm-like term. From this point of view it would be very interesting to simulate H-mode discharges in small experiments where the Bohm-like model is much less important than in large machines.

Furthemore we point out that the non-local modification of transport properties at the L-H transition is stronger near the plasma edge and nearly absent at the plasma centre, and that ρ^* scaling experiments in DIIID carried out for ELMy H-mode discharges have shown transport properties to be gyro-Bohm-like for both ions and electrons: these peculiarities can be easily understood in terms of the mixed model with reduced Bohm-like term.

In fact the Bohm-like term in the mixed model is strongly increasing towards the plasma edge due to the dependence on plasma current through the q^2 term. The gyro-Bohm-like term on the other hand is not increasing or even decreasing near the plasma edge, because the current dependence is absent and it contains an additional dependence on $T_e^{1/2}$ through ρ^* which is decreasing at the edge. As a result of this the gyro-Bohm-like term is dominant in the plasma centre while the Bohm-like term is dominant at the edge. In this way a sudden reduction of the Bohm-like term can naturally describe the reduction of the plasma diffusivity over wide regions of the outer plasma column as it has been observed in JET [17]. Because of the reduction in the Bohm-like term, the modified mixed model would become predominantly gyro-Bohm-like after the transition in agreement with the DIIID results [8] indicating transport properties to be gyro-Bohm-like in H-mode.

We can conclude that the mixed model, tested successfully on L-mode discharges, also represents a good starting point for the development of a transport model unifying the L and H-mode regimes.

6. ACKNOWLEDGEMENTS

We gratefully acknowledge the collaboration of R.E. Waltz, C. Roach and O. Kardaun who provided the data necessary to carry out predictive simulations for discharges of the DIIID, START and ASDEX experiments.

7. REFERENCES

[1] Connor J.W., et al., "Validation of 1-D Transport Models for simulating ITER", Sixteenth IAEA Fusion Energy Conference, Montreal, Canada, 7-11 October 1996, F1-CN-64/FP-21.

[2] Erba M., E. Springmann, A. Taroni, F. Tibone, "Simulation of L-mode Tokamak Discharges and ITER Performance with Energy Transport Coefficients of Bohm and Gyro-Bohm Type", in Local Transport Studies in Fusion Plasmas, J.D. Callen, G. Gorini and E. Sindoni (Eds.), SIF, Bologna 1993, p.39.

[3] Kardaun O., Max-Planck-Institut fur Plasmaphysik, Garching, Private Communication.

[4] Connor J.W., et al., Proceedings of the 22nd EPS Conference on Controlled Fusion and Plasma Physics, Bournemouth (1995), Volume 19 C, Part II, p. 205.

[5] Connor J.W. and Taylor J.B., Nucl. Fus. **17** (1977) 1047.

[6] Krall N.A. and Rosenbluth M.N., Phys. Fluids 8 (1965) 1488.

[7] Connor J.W., et al., Proc. Roy. Soc. London Ser. A 365 (1979) 1.

[8] Petty C.C., et al., Phys. Plasmas **2** (1995) 2342.

[9] Taroni A., M. Erba, E. Springmann and F. Tibone, Plasma Phys. Control Fus. **36** (1994) 1629.

[10] Christiansen J.P., et al., Nucl. Fusion **33** (1993) 863.

[11] Perkins F.W., et al., Phys. Fluids B, **5** (1993) 477.

[12] Erba M., Parail V., Springmann E., Taroni A., Plasma Phys. Control. Fusion **37** (1995) 1249.

[13] Waltz R.E., 1995, private communication.

[14] Balet B., Cordey J.G., Stubberfield P.M., Plasma Phys. Control Fusion **34** (1992) 3.

[15] Waltz R.E., DeBoo J.C., Osborne T.H., Nucl. Fus. **32** (1992) 1051.

[16] Cenacchi G., Taroni A., "JETTO : a Free-Bundary Plasma Transport Code (Basic Version)", Rapporto ENEA RT/TIB 88(5) 1988.

[17] Parail V., et al., "The Physics of L and H-mode confinement in JET", 15th Int. Conf. on Plasma Phyics and Contr. Nucl. Fus. Res., Seville, Spain (1994), Vol. I, p.255.

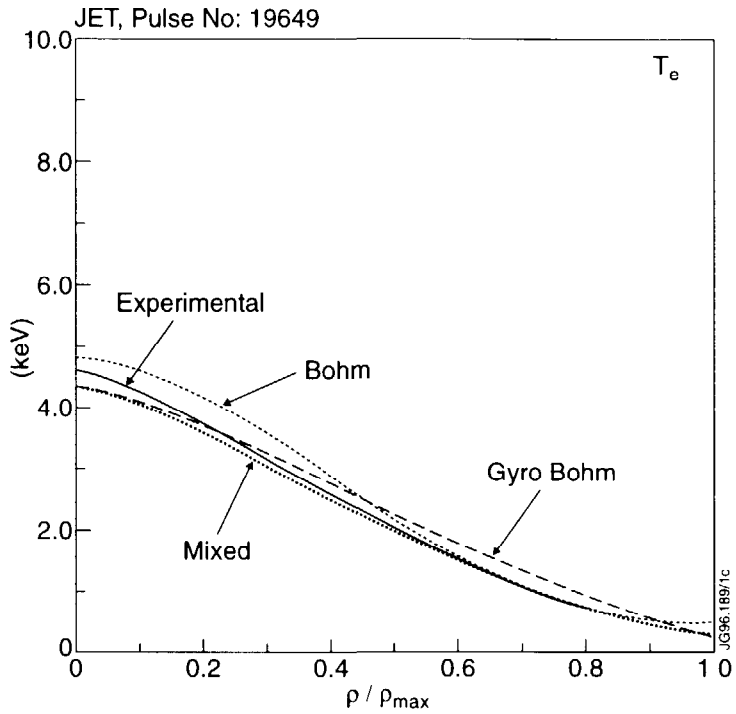

Fig.1a): Comparison of the experimental electron temperature profile (solid line) with the computed electron temperature profiles using the Bohm-like model (small dash), gyro-Bohm-like model (large dash) and mixed model (dotted line) for the JET shot 19649.

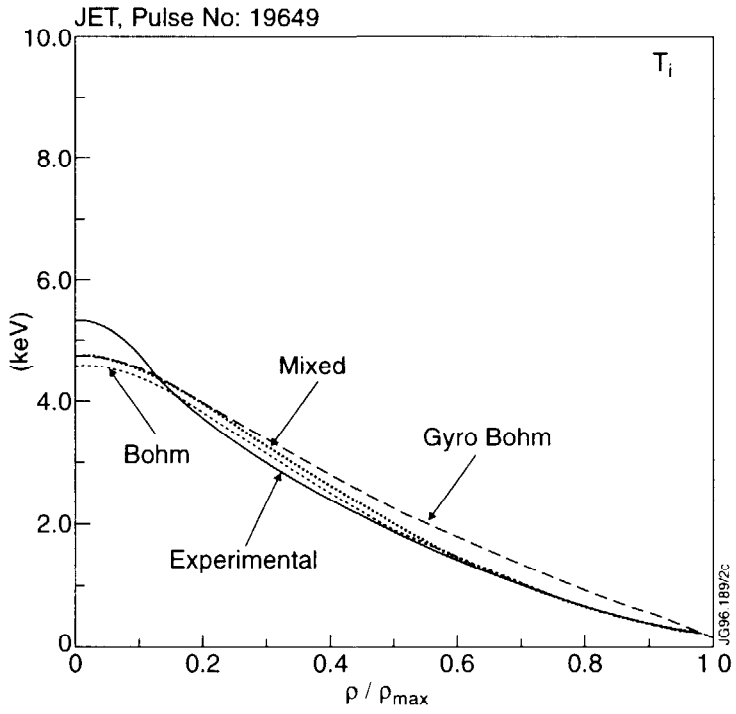

Fig.1b): Comparison of the experimental ion temperature profile (solid line) with the computed ion temperature profiles using the Bohm-like model (small dash), gyro-Bohm-like model (large dash) and mixed model (dotted line) for the JET shot 19649.

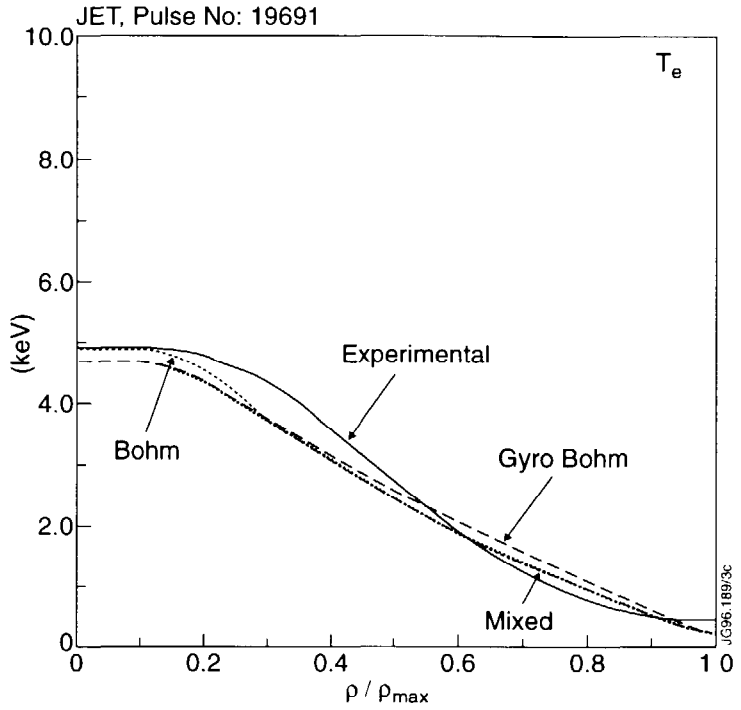

Fig.2a): Comparison of the experimental electron temperature profile (solid line) with the computed electron temperature profiles using the Bohm-like model (small dash), gyro-Bohm-like model (large dash) and mixed model (dotted line) for the JET shot 19691.

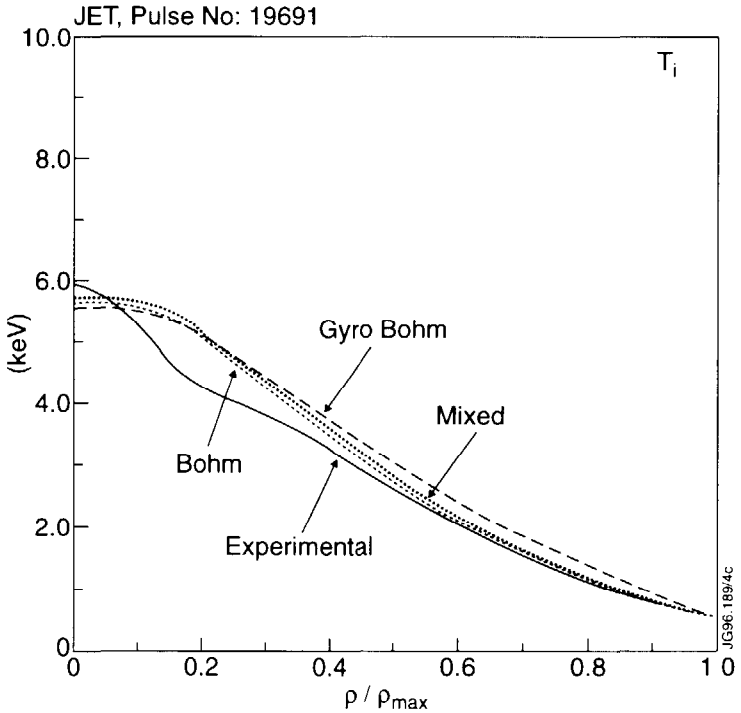

Fig.2b): Comparison of the experimental ion temperature profile (solid line) with the computed ion temperature profiles using the Bohm-like model (small dash), gyro-Bohm-like model (large dash) and mixed model (dotted line) for the JET shot 19691.

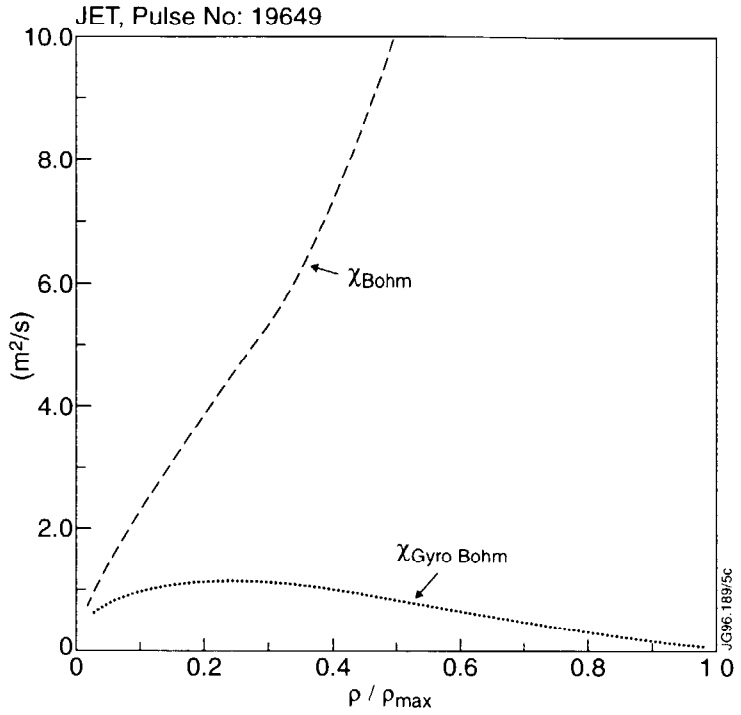

Fig.3): Radial profile of the diffusivity for the Bohm-like part and gyro-Bohm-like part of the mixed model for the JET shot 19649.

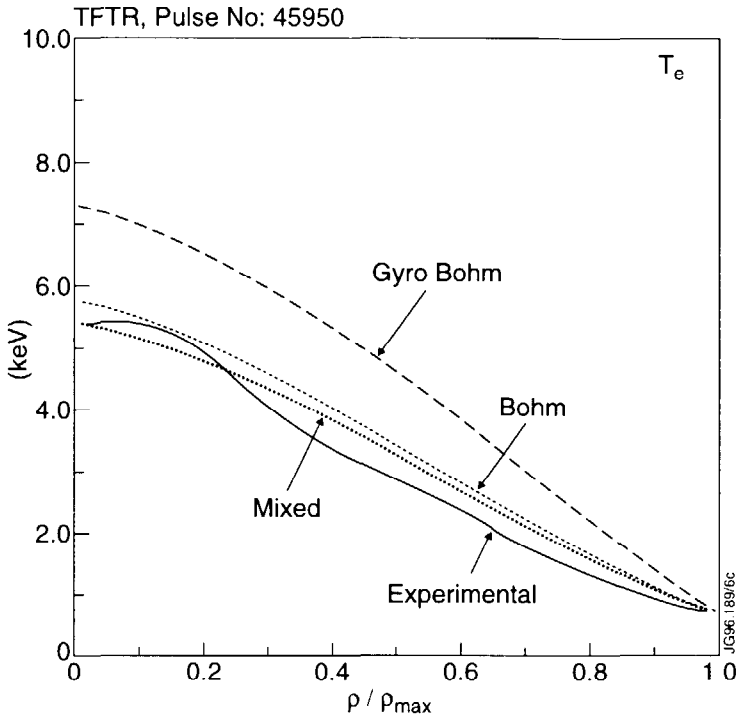

Fig.4a): Comparison of the experimental electron temperature profile (solid line) with the computed electron temperature profiles using the Bohm-like model (small dash), gyro-Bohm-like model (large dash) and mixed model (dotted line) for the TFTR shot 45950.

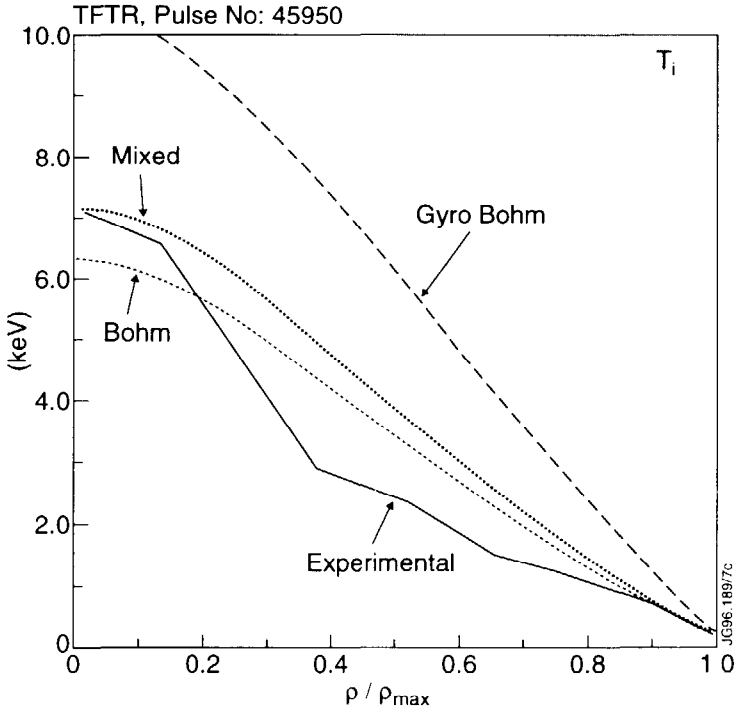

Fig.4b): Comparison of the experimental ion temperature profile (solid line) with the computed ion temperature profiles using the Bohm-like model (small dash), gyro-Bohm-like model (large dash) and mixed model (dotted line) for the TFTR shot 45950.

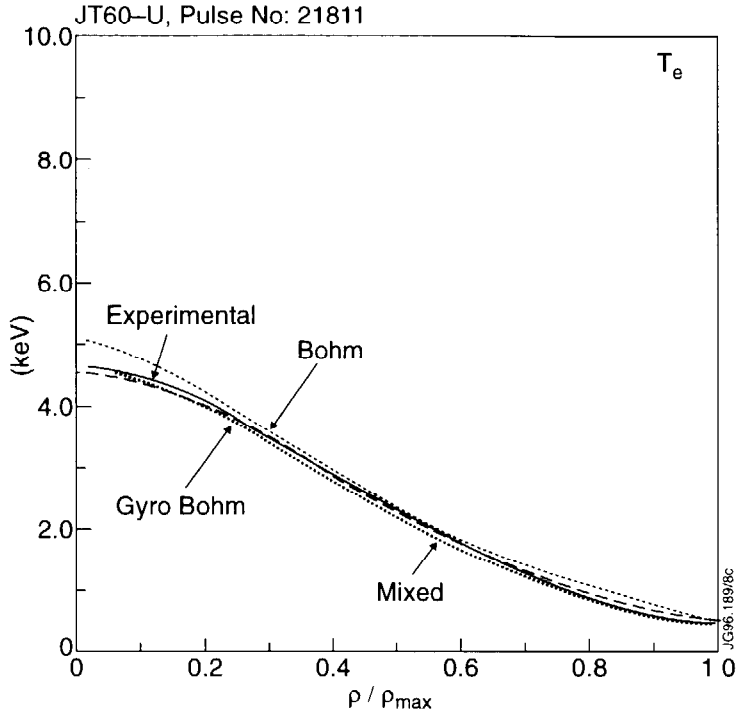

Fig.5a): Comparison of the experimental electron temperature profile (solid line) with the computed electron temperature profiles using the Bohm-like model (small dash), gyro-Bohm-like model (large dash) and mixed model (dotted line) for the JT60-U shot 21811.

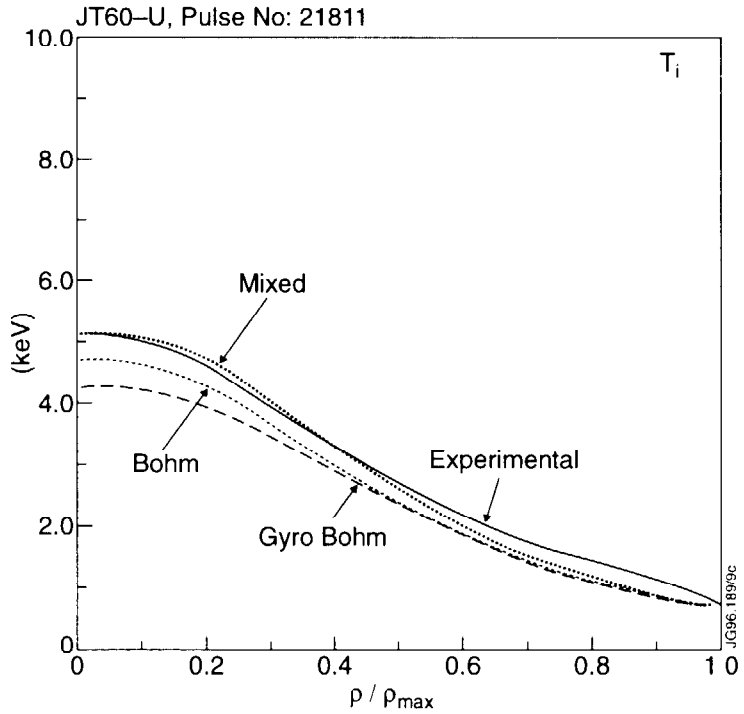

Fig.5b): Comparison of the experimental ion temperature profile (solid line) with the computed ion temperature profiles using the Bohm-like model (small dash), gyro-Bohm-like model (large dash) and mixed model (dotted line) for the JT60-U shot 21811.

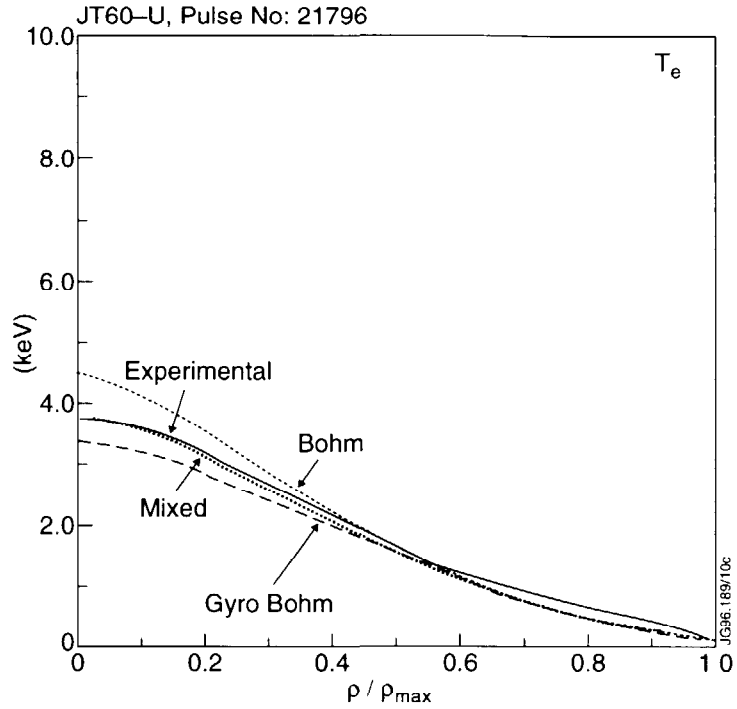

Fig.6a): Comparison of the experimental electron temperature profile (solid line) with the computed electron temperature profiles using the Bohm-like model (small dash), gyro-Bohm-like model (large dash) and mixed model (dotted line) for the JT60-U shot 21796.

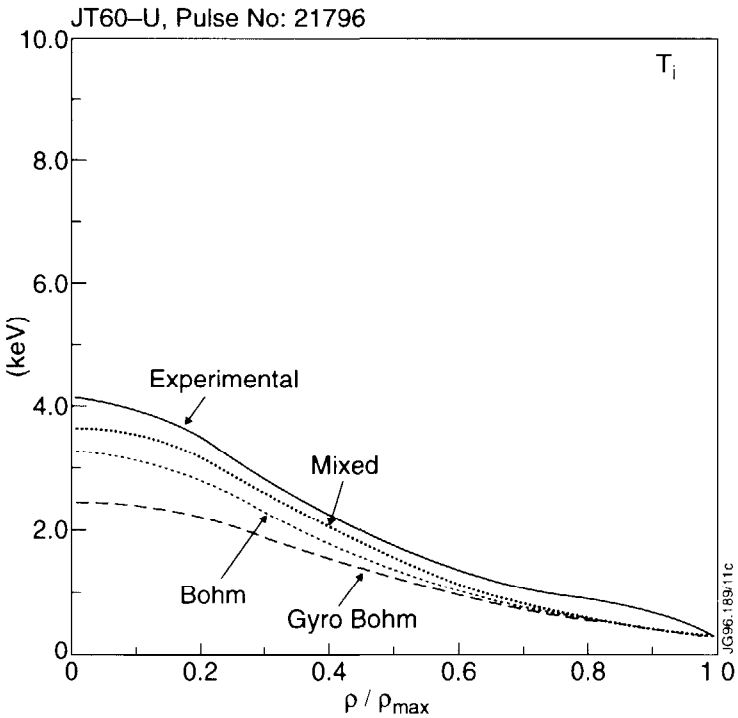

Fig.6b): Comparison of the experimental ion temperature profile (solid line) with the computed ion temperature profiles using the Bohm-like model (small dash), gyro-Bohm-like model (large dash) and mixed model (dotted line) for the JT60-U shot 21796.

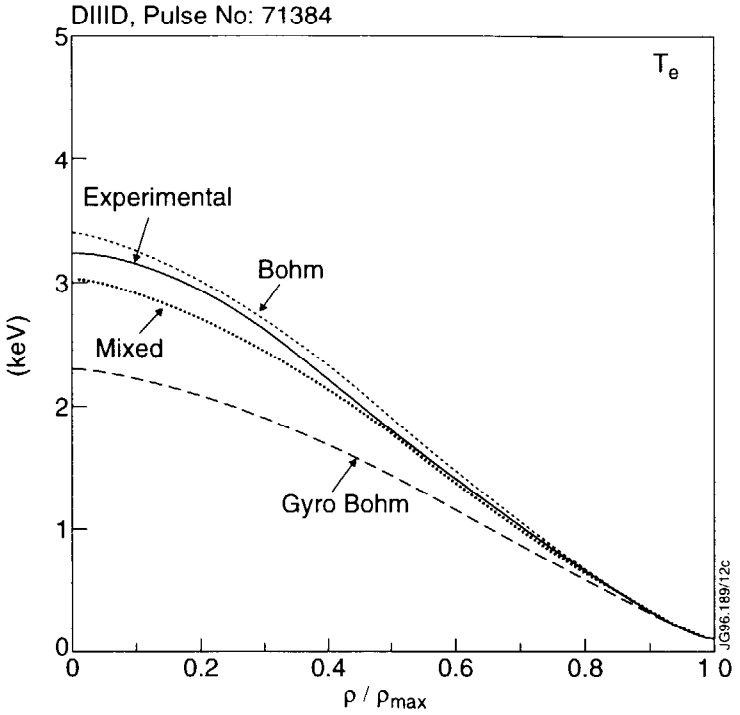

Fig.7a): Comparison of the experimental electron temperature profile (solid line) with the computed electron temperature profiles using the Bohm-like model (small dash), gyro-Bohm-like model (large dash) and mixed model (dotted line) for the DIIID shot 71384.

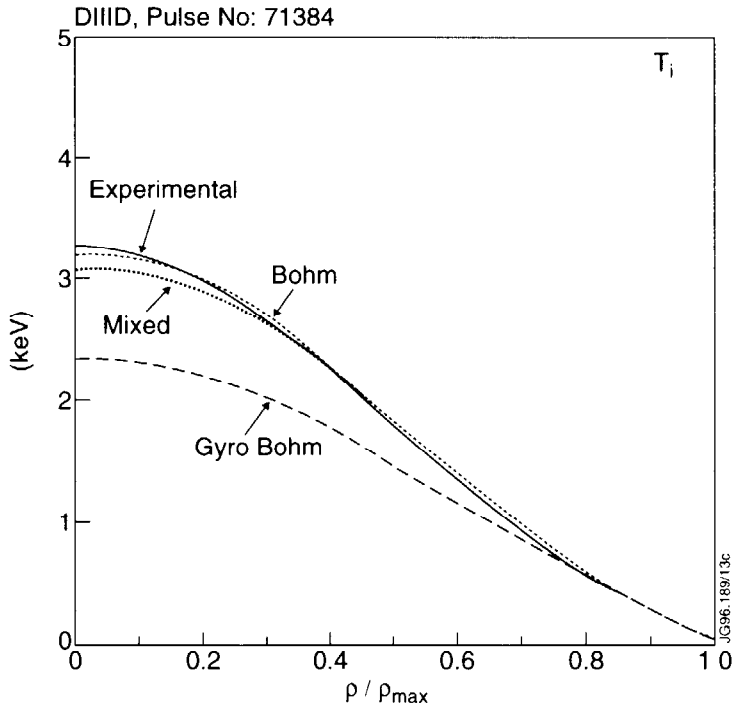

Fig.7b): Comparison of the experimental ion temperature profile (solid line) with the computed ion temperature profiles using the Bohm-like model (small dash), gyro-Bohm-like model (large dash) and mixed model (dotted line) for the DIIID shot 71384.

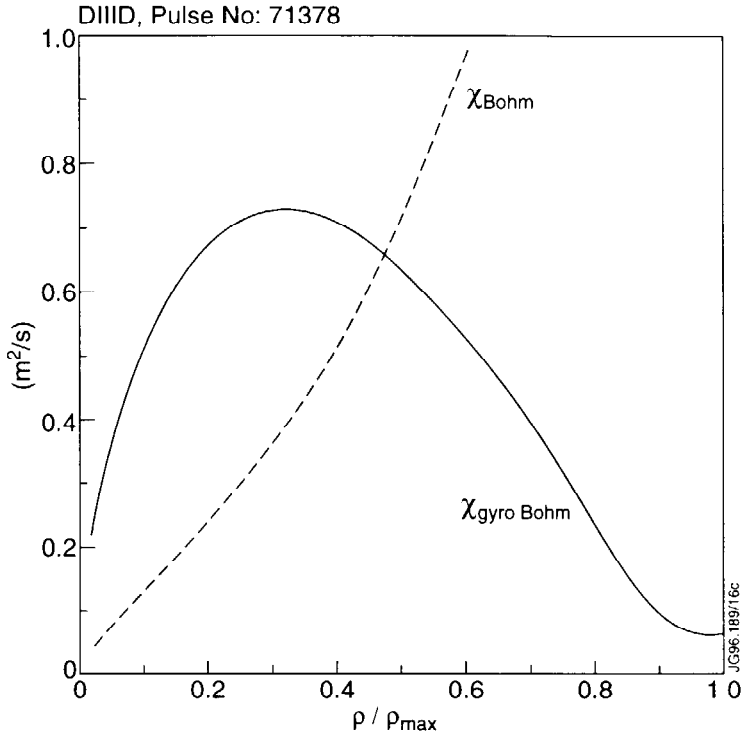

Fig.8): Radial profile of the diffusivity for the Bohm-like part and gyro-Bohm-like part of the mixed model for the DIIID shot 71378.

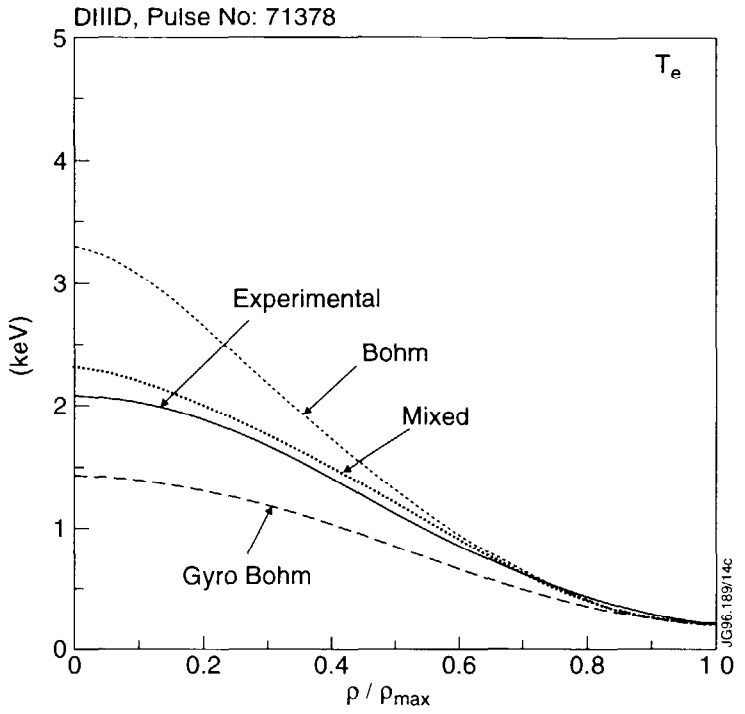

Fig.9a): Comparison of the experimental electron temperature profile (solid line) with the computed electron temperature profiles using the Bohm-like model (small dash), gyro-Bohm-like model (large dash) and mixed model (dotted line) for the DIIID shot 71378.

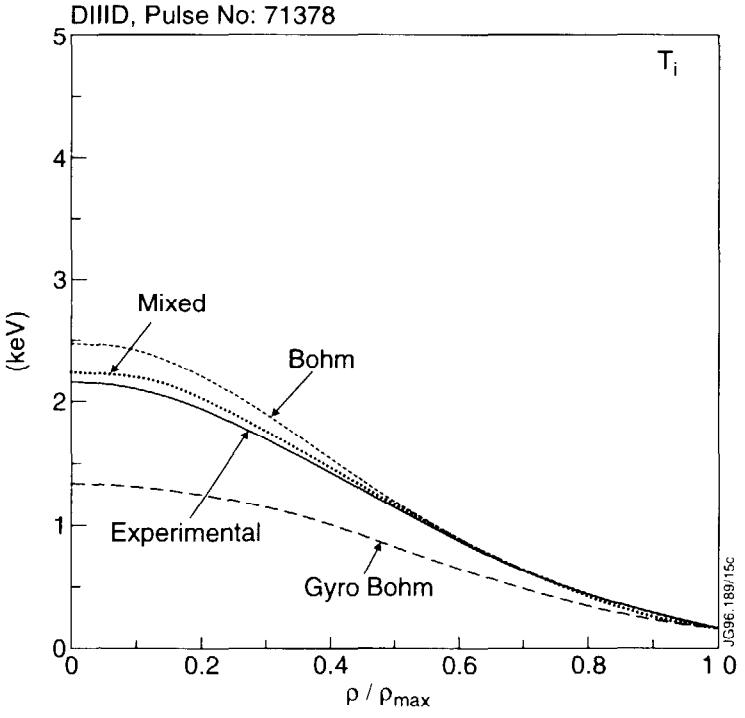

Fig.9b): Comparison of the experimental ion temperature profile (solid line) with the computed ion temperature profiles using the Bohm-like model (small dash), gyro-Bohm-like model (large dash) and mixed model (dotted line) for the DIIID shot 71378.

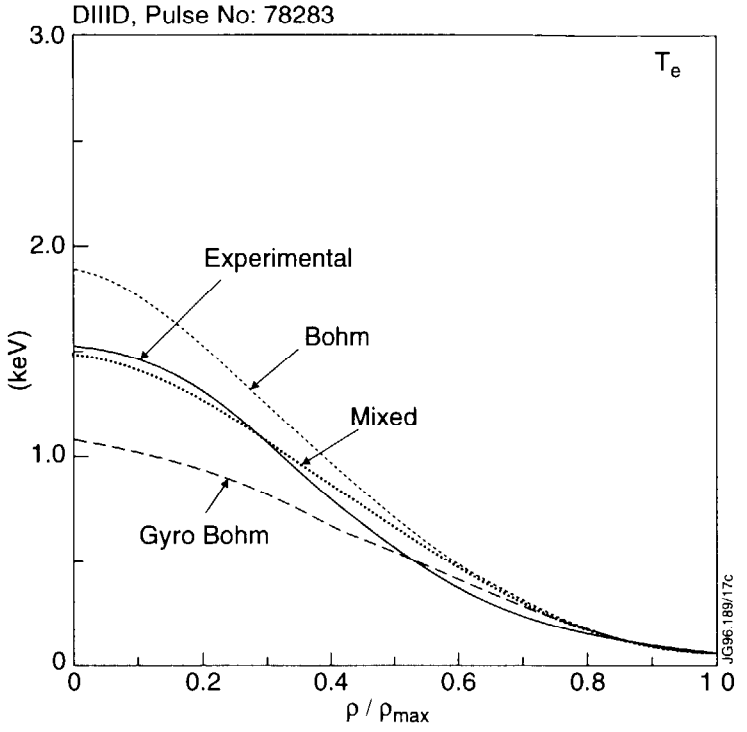

Fig.10a): Comparison of the experimental electron temperature profile (solid line) with the computed electron temperature profiles using the Bohm-like model (small dash), gyro-Bohm-like model (large dash) and mixed model (dotted line) for the DIIID shot 78283.

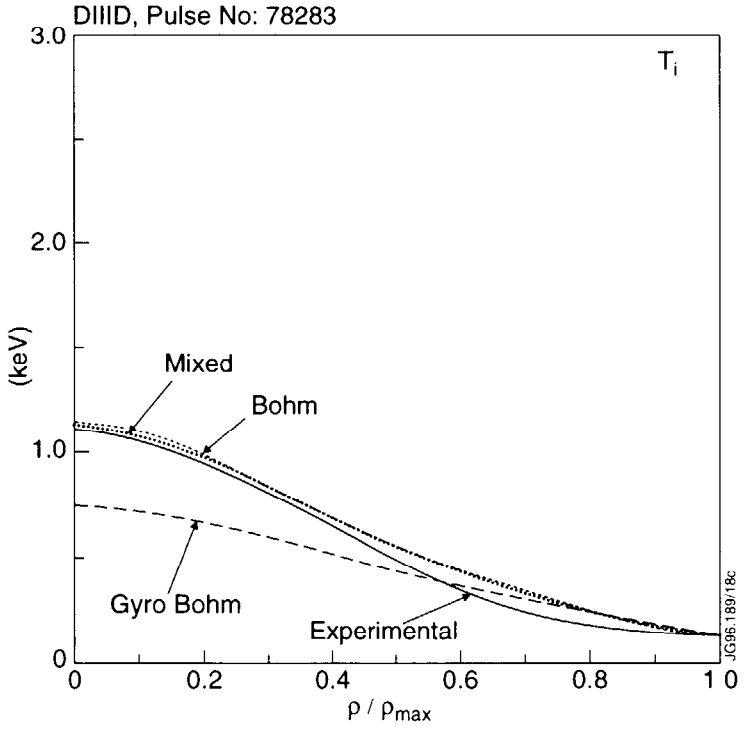

Fig.10b): Comparison of the experimental ion temperature profile (solid line) with the computed ion temperature profiles using the Bohm-like model (small dash), gyro-Bohm-like model (large dash) and mixed model (dotted line) for the DIIID shot 78283.

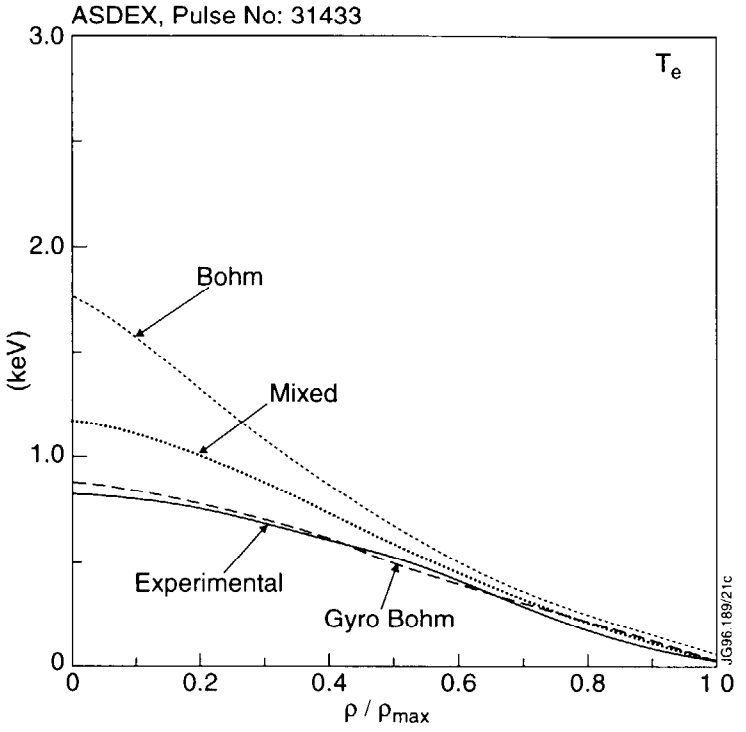

Fig.11): Comparison of the experimental electron temperature profile (solid line) with the computed electron temperature profiles using the Bohm-like model (small dash), gyro-Bohm-like model (large dash) and mixed model (dotted line) for the ASDEX shot 31433.

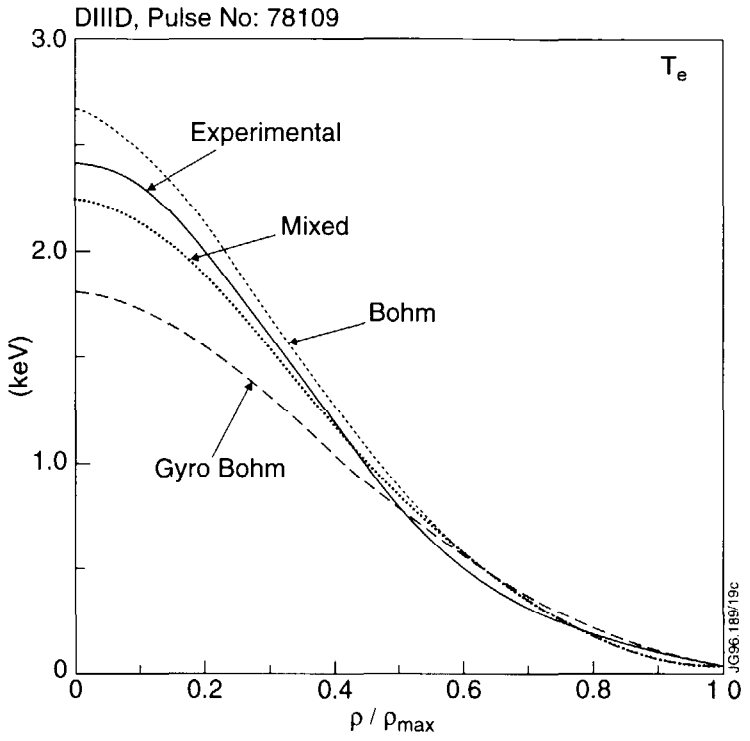

Fig.12a): Comparison of the experimental electron temperature profile (solid line) with the computed electron temperature profiles using the Bohm-like model (small dash), gyro-Bohm-like model (large dash) and mixed model (dotted line) for the DIIID shot 78109.

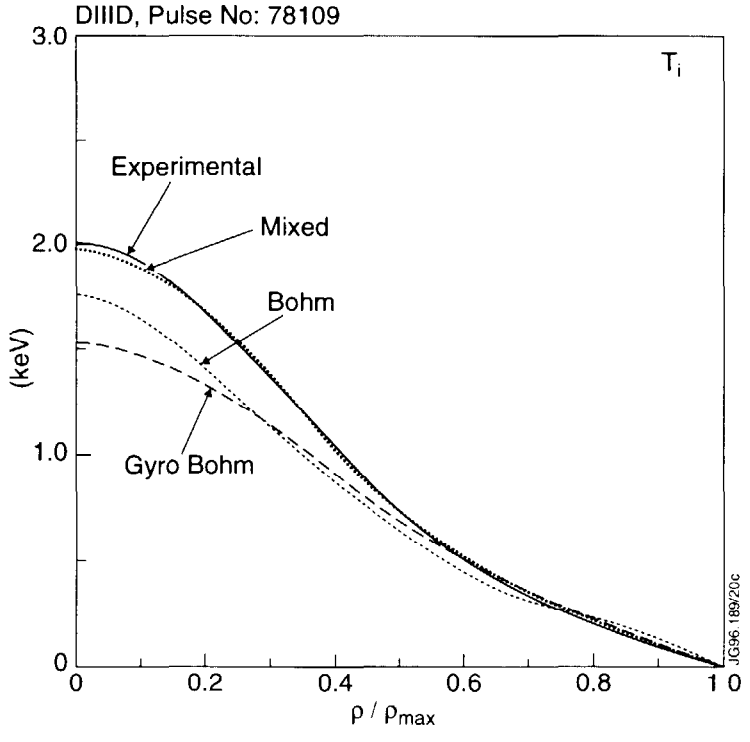

Fig.12b): Comparison of the experimental ion temperature profile (solid line) with the computed ion temperature profiles using the Bohm-like model (small dash), gyro-Bohm-like model (large dash) and mixed model (dotted line) for the DIIID shot 78109.

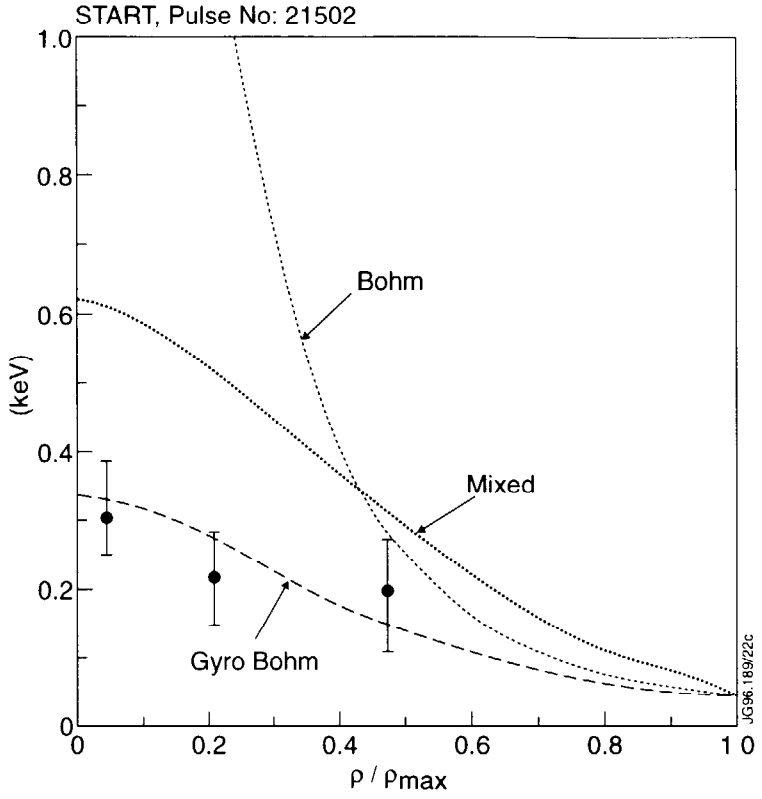

Fig.13): Comparison of the experimental radial measurements of electron temperature (error bars) with the computed electron temperature profiles using the Bohm-like model (small dash), gyro-Bohm-like model (large dash) and mixed model (dotted line) for the START shot 21502.

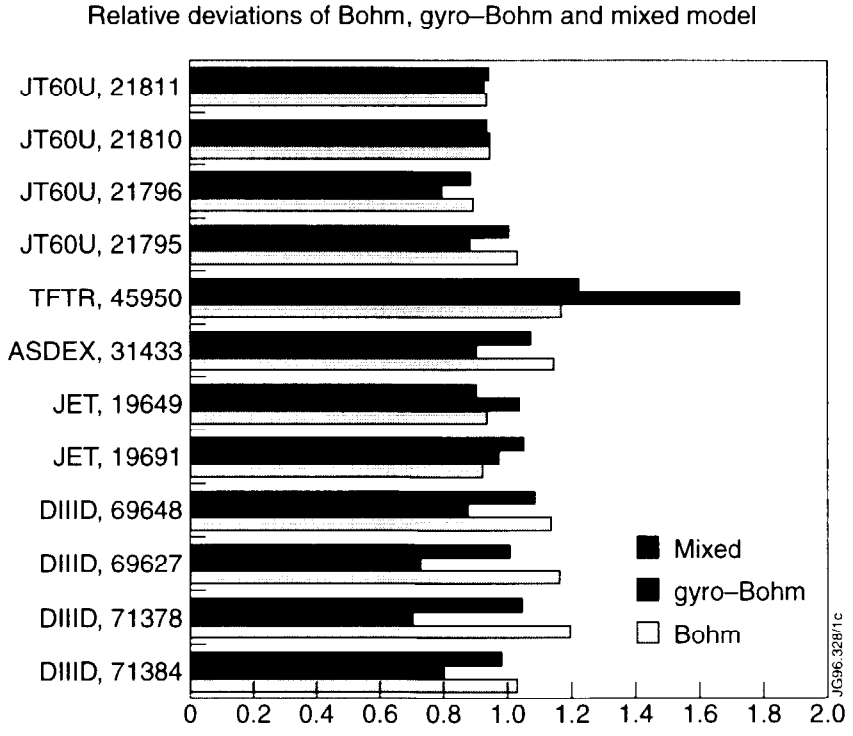

Fig.14): Relative deviations of the thermal energy predicted by the Bohm-like, gyro-Bohm-like and mixed models with respect to the experimental thermal energy for L-mode shots from JT60-U, TFTR, JET and DIIID.